Targeted deletion of the mitogen-activated protein kinase kinase 4 gene in the nervous system causes severe brain developmental defects and premature death

MOLECULAR AND CELLULAR BIOLOGY, Nov. 2007, p. 7935–7946 Vol. 27, No. 22
0270-7306/07/$08.00+0 doi:10.1128/MCB.00226-07

Targeted Deletion of the Mitogen-Activated Protein Kinase Kinase 4 Gene in the Nervous System Causes Severe Brain Developmental Defects and Premature Death▽†

Xin Wang,[1] Bagirathy Nadarajah,[1] Andrew C. Robinson,[1] Barry W. McColl,[1] Jia-Wei Jin,[1] Federico Dajas-Bailador,[1] Raymond P. Boot-Handford,[1,2] and Cathy Tournier[1]*

Faculty of Life Sciences[1] and Wellcome Trust Center for Cell-Matrix Research,[2] University of Manchester, Michael Smith Building, Oxford Road, Manchester M13 9PT, United Kingdom

Received 7 February 2007/Returned for modification 29 March 2007/Accepted 24 August 2007

The c-Jun NH_2-terminal protein kinase (JNK) is a mitogen-activated protein kinase (MAPK) involved in the regulation of various physiological processes. Its activity is increased upon phosphorylation by the MAPK kinases MKK4 and MKK7. The early embryonic death of mice lacking an *mkk4* or *mkk7* gene has provided genetic evidence that MKK4 and MKK7 have nonredundant functions in vivo. To elucidate the physiological role of MKK4, we generated a novel mouse model in which the *mkk4* gene could be specifically deleted in the brain. At birth, the mutant mice were indistinguishable from their control littermates, but they stopped growing a few days later and died prematurely, displaying severe neurological defects. Decreased JNK activity in the absence of MKK4 correlated with impaired phosphorylation of a subset of physiologically relevant JNK substrates and with altered gene expression. These defects resulted in the misalignment of the Purkinje cells in the cerebellum and delayed radial migration in the cerebral cortex. Together, our data demonstrate for the first time that MKK4 is an essential activator of JNK required for the normal development of the brain.

The c-Jun NH_2-terminal protein kinase (JNK) (also called stress-activated protein kinase) is a member of the mitogen-activated protein kinase (MAPK) family, implicated in the regulation of numerous cellular functions in response to environmental stresses, growth factors, hormones, and proinflammatory cytokines (11). Three genes, *jnk1*, *jnk2*, and *jnk3*, encoding 10 isoforms, have been cloned. JNK1 and JNK2 are ubiquitously expressed, while JNK3 is almost exclusively found in the central nervous system (CNS). To understand the physiological functions of the JNK isoforms in vivo, transgenic mice deficient in one or more of the *jnk* genes have been studied (11). Their phenotypic analysis highlighted the importance of JNK-mediated apoptosis during the development of the CNS and in response to brain injury (26, 43, 52). However, apoptosis does not represent the only functional consequence of JNK activation. For example, JNK1 appears to contribute to establishing dendritic architecture in the brain (3, 8, 42).

Analogous to other MAPKs, JNK is activated via the sequential activation of protein kinases, which include two dual-specificity MAPK kinases (MKK4 and MKK7) and multiple MAPK kinase kinases (MEKKs) (51). The MEKKs phosphorylate and activate MKK4 and MKK7, which, in turn activate JNK by dual phosphorylation on Thr and Tyr residues within a Thr-Pro-Tyr motif in protein kinase subdomain VIII (51). While MKK7 is a specific activator of JNK, MKK4 can also phosphorylate the Thr-Gly-Tyr motif of the p38 MAPK (50). Like JNK, p38 MAPK is activated in mammalian cells by various stress stimuli and proinflammatory cytokines (55). Physiological evidence for a role of MKK4 in activating the p38 MAPK cascade was recently provided by demonstrating that decreased expression of MKK4 due to small interfering RNA in mouse embryonic fibroblasts lacking both MKK3 and MKK6 suppressed stress-induced p38 MAPK activation (5).

Similar to the early embryonic death caused by the targeted deletion of both *jnk1* and *jnk2* genes (26, 43), mice null for *mkk4* or *mkk7* die before birth (50). The nonredundant functions of MKK4 and MKK7 in vivo may be due to their distinct tissue distributions and subcellular localizations. For example, in neurons, MKK4 is present in both the cell body and the processes (dendrites and axons), while MKK7 is almost exclusively detected in the nucleus (10). Consequently, MKK4 is more likely to be critical in maintaining the high basal activity of JNK in neurites. By enabling JNK to phosphorylate cytosolic targets, such as microtubule-associated proteins (MAPs), MKK4 may have a prominent role in mediating the effect of JNK on dendritic outgrowth and the establishment of functional neural circuits in the brain (3, 8, 42).

To advance our knowledge of the biological function of MKK4 in the nervous system, we developed a novel mouse model displaying a specific deletion of the *mkk4* gene in the CNS. Phenotypic analysis of the mice indicated that the deletion of the *mkk4* gene affects the normal development of the brain. Decreased basal JNK activity associated with the absence of MKK4 causes irregular alignment of Purkinje cells in the cerebellum and delayed radial migration in the cortex. The identification of a subset of physiologically relevant substrates of JNK whose phosphorylation required MKK4 and MKK4 target genes will greatly contribute to unraveling the cell-signaling mechanisms involved during brain development.

* Corresponding author. Mailing address: Faculty of Life Sciences, University of Manchester, Michael Smith Building, Oxford Road, Manchester M13 9PT, United Kingdom. Phone: 44 161 275 5417. Fax: 44 161 275 5082. E-mail: cathy.tournier@manchester.ac.uk.

† Supplemental material for this article may be found at http://mcb.asm.org/.

▽ Published ahead of print on 17 September 2007.

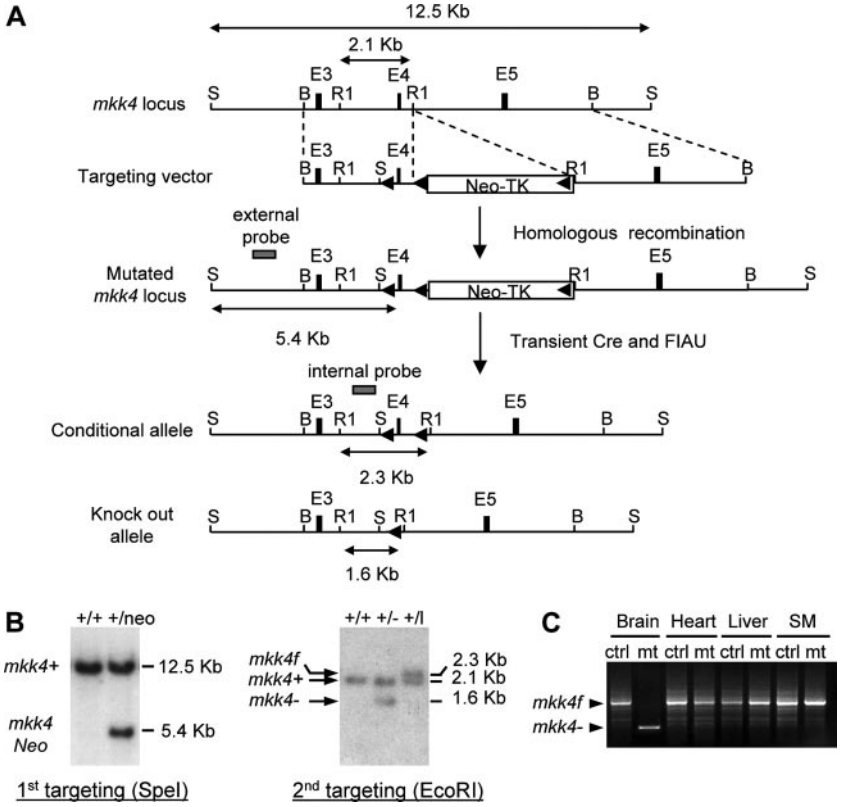

FIG. 1. Strategy for the mutation of the *mkk4* gene. (A) The genomic region at the *mkk4* locus, the *mkk4* targeting vector, and the predicted structure of the mutated *mkk4* gene are depicted. Restriction enzyme sites are indicated (B, BamHI; R, EcoRI; S, SpeI). The black boxes are *mkk4* exons. The open box is the neomycin-thymidine kinase cassette (Neo-TK). The black arrowheads indicate the positions of the *loxP* sites. (B) Southern blotting analysis of SpeI- and EcoRI-restricted genomic DNA prepared from ES cell clones indicated the presence of all expected genotypes. The blots were probed with random-primed ^{32}P-labeled mouse MKK4 genomic external and internal probes (gray box in panel A). (C) Genomic DNAs isolated from brains, hearts, livers, and skeletal muscles (SM) of 1-week-old mice were amplified by PCR with primers specific for the *mkk4* gene. *mkk4+*, *mkk4Neo*, *mkk4f*, and *mkk4−* correspond to the wild-type, mutated, conditional, and knockout alleles, respectively. ctrl, control; mt, mutant.

MATERIALS AND METHODS

Generation of *mkk4-flox* mice. The sequence of the *mkk4* gene locus was obtained from GenBank (accession no. AL663069). Gene analysis revealed that the *mkk4* gene is composed of 11 exons and 10 introns. An 8.2-kb BamHI genomic fragment encompassing exons 3, 4, and 5 of the *mkk4* gene was isolated from an RPCI-21 PAC library (United Kingdom HGMP Resource Centre) and subcloned into the pBluescript II KS vector (Stratagene). A double-stranded oligonucleotide containing a SpeI site and a LoxP site was inserted into a SpeI site created 5′ to exon 4, and a *loxP-neo*-internal ribosome entry site-*tk-loxP* cassette was inserted into the EcoRI site 3′ of the same exon. This gave rise to a targeting vector comprising 2.8-kb BamH1-EcoRI and 5.3-kb EcoRI-BamHI fragments of MKK4-homologous sequences at its 5′ and 3′ extremity, respectively (Fig. 1). Embryonic stem (ES) cell transfection, selection, and screening were carried out as described previously (34), using a probe located outside of the 5′ region of the targeting vector (Fig. 1). Three positive clones were retransfected with a Cre-expressing plasmid and counterselected in 1-(2-deoxy-2-fluoro-β-D-arabinofuranosyl)-5-iodouracil (FIAU), and clones that had retained two *loxP* sites flanking exon 4 were identified by Southern blotting using a probe located inside of the targeting vector (Fig. 1). Germ line-transmitting chimeras were generated. All mice employed for this study were hosted in a pathogen-free facility at the University of Manchester. The animal studies were carried out according to Home Office and institutional guidelines.

Genotype determination of mice and tissues. Offspring carrying the *mkk4-flox* allele were identified by PCRs on tail DNA using forward (5′-GACATTGAGT TCCT TGCG-3′) and reverse (5′-TCCTATGTAGTAGGAGTTTG-3′) primers. Fragments (390 bp and 490 bp) were amplified from the wild-type and *mkk4-flox* alleles, respectively. The *nestin-Cre* transgene was identified by PCR as previously described (18). Genotype determination of tissues was performed by PCR on genomic DNA using forward (5′-TCCTATGTAGTAGGAGTTTG-3′) and reverse (5′-GGCAGCTTGTCAGATG-3′) primers. Fragments (950 bp and 450 bp) were amplified from the *mkk4-flox* and disrupted alleles, respectively.

Preparation of lysates. Proteins were extracted from tissues in Triton lysis buffer (20 mM Tris, pH 7.4, 137 mM NaCl, 2 mM EDTA, 1% Triton X-100, 25 mM β-glycerophosphate, 10% glycerol, 1 mM orthovanadate, 1 mM phenylsulfonyl fluoride, 10 μg/ml leupeptin, 10 μg/ml aprotinin). Extracts were clarified by centrifugation (14,000 × *g* for 10 min at 4°C). The concentrations of soluble proteins in the supernatants were quantified by the Bradford method (Bio-Rad).

Immunoblot analysis. Extracts (20 μg) were resolved by sodium dodecyl sulfate-polyacrylamide gel electrophoresis (SDS-PAGE) (10% or 8% polyacrylamide gels) and electrophoretically transferred to Immobilon-P membranes (Millipore, Inc.). The membranes were incubated with 3% nonfat dry milk at 4°C for 30 min and probed overnight with antibodies (1:1,000) to MKK4 (BD Pharmingen), MKK7 (BD Pharmingen), JNK (Santa Cruz), p38 MAPK (Santa Cruz), tubulin (Sigma), MAP1B (Santa Cruz), the neurofilament heavy-chain protein (NF-H) (Sigma), and phosphorylated epitopes of MAP1B and NF-H (Covance; SMI31). Immune complexes were detected by enhanced chemiluminescence with anti-mouse or anti-rabbit immunoglobulin G coupled to horseradish peroxidase as the secondary antibody (Amersham-Pharmacia).

Protein kinase assay. JNK and p38 MAPK activities were measured in lysates following incubation with glutathione *S*-transferase (GST)–c-Jun and glutathione-Sepharose beads or with a polyclonal antibody to p38 MAPK (36) and protein A agarose beads, respectively, for 2 to 3 h at 4°C. Complexes were washed three times with Triton lysis buffer and twice with kinase buffer (25 mM HEPES, pH 7.4, 25 mM β-glycerophosphate, 25 mM $MgCl_2$, 2 mM dithiothreitol, 0.1% orthovanadate) prior to being incubated at 30°C for 20 min in kinase buffer

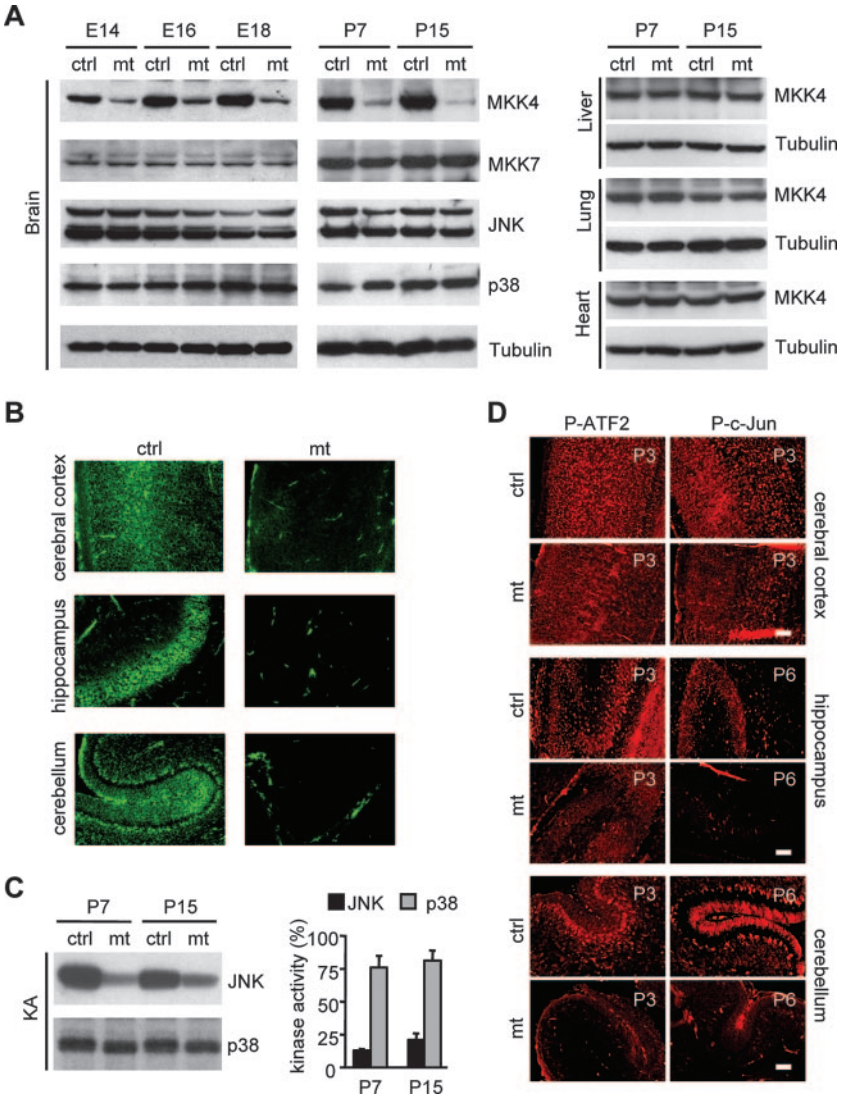

FIG. 2. The disruption of the *mkk4* gene significantly reduces JNK activity. (A) Tissue extracts prepared from embryos and mice at various ages that were homozygous for the *mkk4-flox* allele and expressed (mutant [mt]) or did not express (control [ctrl]) Cre were analyzed for MKK4, MKK7, JNK, and p38 MAPK expression by immunoblot analysis using specific polyclonal antibodies. The detection of tubulin expression was performed to monitor protein loading. (B) The inactivation of the *mkk4* gene in the brains of the mutant mice was confirmed by immunostaining of sagittal sections of the cerebral cortex, the hippocampus, and the cerebellum at P6 with an antibody to MKK4. (C) Endogenous JNK and p38 MAPK activities were measured by protein kinase assay (KA) in the presence of [γ-^{32}P]ATP. The radioactivity incorporated into GST-cJun or GST-ATF2 was quantitated after SDS/PAGE by phosphorimager analysis. The data correspond to the means and standard errors of three independent experiments. (D) Sagittal sections of different areas of control and mutant brains at P3 or P6 were immunostained with antibodies to phospho-c-Jun (Ser63) and phospho-ATF2 (Thr71). The results demonstrate that the loss of MKK4 prevents the phosphorylation of c-Jun and ATF2 in the nervous system.

containing 50 μM [γ-^{32}P]ATP (10 Ci/mmol) and 1 μg of GST-activating transcription factor 2 (ATF2) for p38 MAPK assays. The reactions were terminated by the addition of Laemmli sample buffer. Proteins were resolved by SDS-PAGE and identified by autoradiography. The incorporation of [^{32}P]phosphate was quantitated by phosphorimager analysis.

Histological and immunohistochemical analyses. Mice were anesthetized and perfused with 0.9% saline, followed by 4% paraformaldehyde. Their brains were removed and fixed in 4% paraformaldehyde overnight at 4°C before being embedded in paraffin. For Nissl staining, 8-μm-thick horizontal sections were stained with 1% cresyl violet (34). For immunohistochemistry, 10-μm sagittal sections were deparaffinized, rehydrated, and treated in boiling sodium citrate buffer (10 mM, pH 6.0) for 10 min to unmask the antigen. Endogenous peroxidase activity was quenched by treating the slides with 3% hydrogen peroxidase for 10 min. Twelve-micrometer horizontal cryosections fixed in ice-cold acetone-methanol for 20 min were used to detect the neural L1 cell adhesion molecule. Sections were blocked in phosphate-buffered saline (PBS) containing 10% goat serum and 0.1% Triton X-100 for 1 h at room temperature prior to being incubated overnight at 4°C with primary antibodies to MKK4 (1:100; BD Pharmingen), phospho-c-Jun (Ser 73) (1:100; Cell Signaling), phospho-ATF2 (Thr 71) (1:100; Cell Signaling), calbindin (1:500; Chemicon), neuronal nuclei (NeuN) (1:500; Chemicon), myelin basic protein (MBP) (1:100; MAB387; Chemicon), nestin (1:100; Developmental Studies Hybridoma Bank), nonphosphorylated epitopes of MAP1B and NF-H (1:500; SMI32; Covance), MAP2 (1:500; Sigma), and L1 (1:50; MAB5272; Chemicon). The following day, the slides were rinsed in PBS and incubated at room temperature in the dark for 1 h with secondary goat anti-mouse, goat anti-rabbit, or donkey anti-rat antibodies conjugated to Alexa Fluoro 488 (1:500; Invitrogen), Alexa Fluoro 568 (1:500; Invitrogen), or fluorescein (1:500; Jackson ImmunoResearch), respectively. The slides were washed

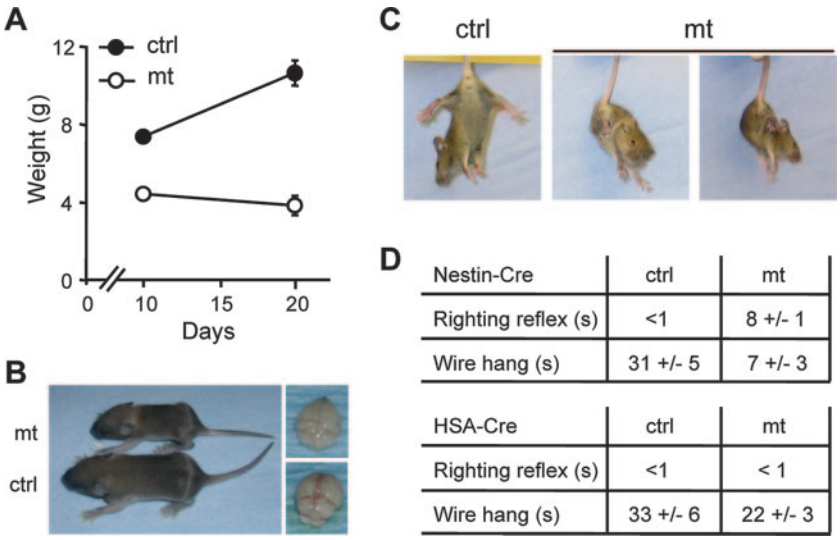

Nestin-Cre	ctrl	mt
Righting reflex (s)	<1	8 +/- 1
Wire hang (s)	31 +/- 5	7 +/- 3

HSA-Cre	ctrl	mt
Righting reflex (s)	<1	< 1
Wire hang (s)	33 +/- 6	22 +/- 3

FIG. 3. Mice lacking MKK4 display abnormal growth and motor deficits. (A) Mutant (mt) mice that lack MKK4 in the brain display severe growth defects, although their weight at birth is indistinguishable from that of control (ctrl) littermates. (B) At P20, the mt mice are notably smaller than the ctrl littermates and display a reduction in brain size accordingly. (C) MKK4-deficient mice display awkward gait when held by the tail. (D) The behaviors of mice homozygous for the *mkk4-flox* allele and harboring a *cre* transgene under the control of the nestin or the human skeletal α-actin (HSA) promoter were compared. Motor balance and muscular strength were examined by righting reflex and wire hang tests, respectively. For the righting reflex test, individual mice were placed on their backs and the latency to turning back onto their feet was scored in each case. For the wire hang test, individual mice were placed on a wire held in an inverted position and the latency to falling off was scored in each case.

three times for 10 min each time in PBS prior to being viewed using the Nikon Eclipse E600 microscope.

Birth date analysis. Time-mated pregnant mice were injected intraperitoneally with bromodeoxyuridine (BrdU) (50 μg/g body weight) at postcoitum day 11, 13, 14, or 16. The offspring were sacrificed at postnatal day 1 (P1) or P7, and their brains were processed for paraffin sectioning. Deparaffinized and rehydrated 10-μm sagittal sections were treated with 2 N HCl at 60°C for 8 min to denature DNA and neutralized with 0.1% boric acid buffer, pH 8.5. After being blocked in PBS containing 5% goat serum, the sections were incubated overnight at 4°C with a mouse monoclonal anti-BrdU antibody (1:100; Progen). BrdU immunoreactivity was detected following incubation of the slides with Alexa Fluoro-conjugated goat anti-mouse antibody (1:500; Invitrogen). The immunofluorescence was detected using a Nikon Eclipse E600 microscope. Fluorescence intensities inside similar-width rectangles in various regions of the cerebral cortex were quantified with MetaMorph software and expressed as average pixel densities.

Real-time quantitative PCR. Total RNA was isolated from embryonic day 14 (E14) forebrains using the Trizol reagent, and cDNA synthesis was carried out as previously described (23). Real-time quantitative PCRs were performed using the SYBR Green I Core Kit (Eurogentec). (For the sequences of the forward and reverse primers, see the supplemental material.) PCR products were detected with the ABI-PRISM 7700 sequence detection system (Applied Biosystems). The results were analyzed using the $2^{-\Delta\Delta CT}$ method (30). The level of expression of mRNA was normalized to glyceraldehyde-3-phosphate dehydrogenase mRNA.

RESULTS

Inactivation of MKK4 in the brain. To make the homozygous *mkk4-flox* mice, a targeting vector was designed to modify the *mkk4* gene by homologous recombination in ES cells, so that exon 4 was flanked by *loxP* sites (Fig. 1A). The *loxP* sites do not interfere with the normal expression of the gene but constitute a binding domain for the DNA recombinase Cre. Thus, the deletion of the *mkk4-flox* gene in a particular cell lineage can be triggered in vivo by crossing the mutant *loxP* mice with transgenic animals expressing tissue-specific Cre (45). An example of a homologous recombined ES cell clone identified by Southern blotting is shown in Fig. 1B. Chimeric mice were generated and bred on the C57BL/6 background for germ line transmission of the mutation. Mice carrying homozygous *mkk4-flox* alleles were healthy and fertile, confirming that the presence of two *loxP* sites did not affect MKK4 function in vivo.

To inactivate *mkk4* in the nervous system, we used a transgenic mouse line that expresses Cre under the control of the nestin promoter (18). The functionality of Cre was tested in vivo by crossing the nestin-Cre mice with mice carrying a LacZ-neomycin phosphotransferase (*Rosa26 lacZ-loxP*) transgene. In this mouse line, β-galactosidase expression is induced following Cre-mediated excision of the *loxP*-flanked DNA sequences in the transgene. Consistent with previous characterizations of the nestin-Cre mice (18), whole-mount staining demonstrated that the nestin-Cre line induces efficient recombination in cells that are committed to the neural lineage (data not shown). Multiple litters of *mkk4-flox* mice were crossed with nestin-Cre animals. Amplification by PCR with primers specific for the *mkk4* gene on genomic DNA isolated from various tissues extracted from 1-week-old mice confirmed the specific recombination of the *mkk4* gene in the brain (Fig. 1C).

Inactivation of MKK4 decreased JNK activity in the nervous system. Immunoblot analysis of brain extracts of littermates homozygous for the *mkk4-flox* allele and expressing Cre demonstrated that the inactivation of the *mkk4* gene in the nervous system occurred as early as E14 (Fig. 2A). Reduction of MKK4 expression in the mutant embryos and mice did not cause any compensatory changes in the expression of MKK7. The remaining low level of MKK4 detected was expected, since MKK4 is likely to be expressed in meningeal cells and blood vessels, where Cre is not active. Immunostaining of sagittal sections of the cerebral cortex, hippocampus, and cerebellum

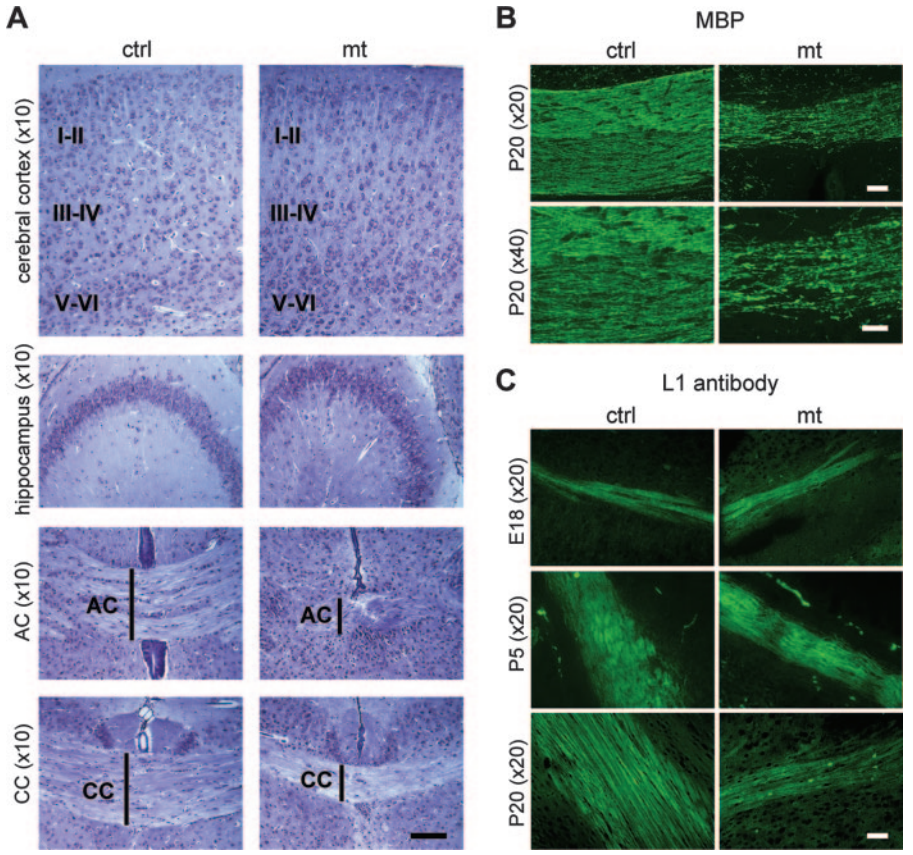

FIG. 4. The loss of MKK4 affects the organization of the fibers of axons forming the CC and the AC. (A) Sagittal sections of adult brains were processed by Nissl staining. The fibers of axons forming the AC and the CC in the mutant brain are less fasciculated and appear disorganized and swollen. (B and C) Sagittal sections of the CC at different embryonic and postnatal stages were stained with antibodies to MBP (B) and L1 (C). The photographs were taken at different magnifications, as indicated. Scale bars: ×10, 100 μm; ×20, 50 μm; ×40, 25 μm.

at P6 with an antibody to MKK4 substantiated the absence of MKK4 in the mutant brain (Fig. 2B). The selective ablation of *mkk4* in the nervous system is demonstrated by similar expression of MKK4 in the livers, lungs, and hearts of both control and mutant mice (Fig. 2A).

No marked difference was observed in the expression levels of JNK and p38 MAPK (Fig. 2A). However, JNK and p38 MAPK activities were decreased by around 80% and 20%, respectively, following the deletion of the *mkk4* gene (Fig. 2C). Consistent with the requirement for JNK and p38 MAPK to transcriptionally activate AP-1 factors (53), this resulted in impaired phosphorylation of c-Jun and ATF2 in the brains of mice lacking MKK4 (Fig. 2D). The areas examined included the cerebral cortex, the hippocampus, and the cerebellum at P3 for phosphorylated ATF2 and at P3 or P6 for phosphorylated c-Jun. Taken together, these results led us to conclude that MKK4 is a critical activator of JNK in the nervous system.

Phenotypic analysis of MKK4 mutant mice. At birth, the mutant mice were indistinguishable from their control littermates, but they stopped growing a few days later and generally died by P21 (Fig. 3A). They became notably smaller by 7 days postpartum, reaching on average 40% of the weight of sex-matched littermates at P20 (Fig. 3A and B). The size of the brain was reduced correspondingly. Between P13 and P15, the mutant mice displayed striking neurological disorders that included ataxia, whole-body tremor, and awkward gait when held by the tail (Fig. 3C). Decreased motor balance and coordination were demonstrated by increased latency of the mutant mice at P14 in turning back onto their feet when placed on their backs (Fig. 3D, righting reflex). The MKK4-deficient mice were also five times less able than the control animals to hold onto a hanging wire (Fig. 3D, wire hang).

To confirm that the abnormal behavior displayed by the MKK4 mutant mice was not a consequence of muscle wasting, we tested the effect of *mkk4* gene deletion on skeletal muscle. Mice homozygous for the *mkk4-flox* allele were crossed with transgenic mice that expressed Cre under the control of the human skeletal α-actin promoter (46). The specific ablation of MKK4 in skeletal muscle was verified by immunoblot analysis (data not shown). The growth curve of the muscle-mutant mice was indistinguishable from that of their littermates (data not shown). Although they were slightly less able than the control mice to hold on to the hanging wire, their righting reflex was normal (Fig. 3D). Collectively, these behavioral studies clearly establish that mice carrying a specific deletion of the *mkk4* gene in the nervous system display motor deficits due to neurological defects.

Mice that lack MKK4 in the CNS display developmental defects in the brain. The role of MKK4 in the developing telencephalon was determined by comparing histological sec-

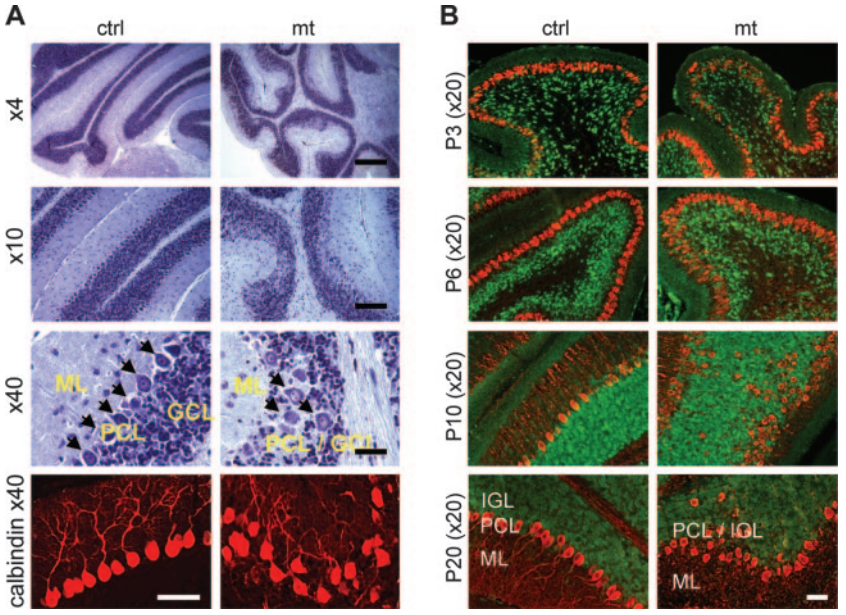

FIG. 5. MKK4 is required for the positioning of the Purkinje cells in the cerebellum. (A) Nissl staining of sagittal sections of the adult cerebellum demonstrates that the Purkinje cells are unable to align beneath the loosely packed IGL. Photographs of the control (ctrl) and mutant (mt) cerebella were taken at different magnifications, as indicated. The arrows mark the aberrant positions of the Purkinje cells in the brain lacking MKK4. Immunostaining of parasaggital sections of the cerebellum at P20 with anticalbindin (red) antibody demonstrates that the loss of MKK4 does not interfere with the maturation of the Purkinje cells. (B) Sagittal sections through cerebellar cortices at various ages were double stained with antibodies against calbindin (red) and NeuN (green) to detect Purkinje cells and granule neurons, respectively. By P10, the sheet of Purkinje cells, several cells thick, had dispersed into a monolayer in the control (ctrl) but not in the mutant (mt) cerebellum. ML, molecular layer. Scale bars: ×4, 250 μm; ×10, 100 μm; ×20, 50 μm; ×40, 25 μm.

tions of control and mutant brains at P20 (Fig. 4). No marked differences were detected in the cerebral cortex and the hippocampus. However, the anterior commissure (AC) and the corpus callosum (CC) in the mutant brain were reduced in thickness, possibly due to less fasciculated, disorganized axons (Fig. 4A). This hypothesis was confirmed by immunostaining saggital sections of the CC at embryonic and postnatal stages with antibodies to MBP, a marker of oligodendrocytes, and to L1, a neural-cell adhesion molecule that is primarily expressed by thalamocortical axons (Fig. 4B and C). In contrast to the control brain, staining of the thalamic axons lacking MKK4 remained diffused at P20, suggesting that defasciculation of the cortical afferents had occurred by the third postnatal week (Fig. 4C).

Similarly, the cerebellum displayed discernible macroscopic abnormalities in the absence of MKK4 that included a loosely packed inner granular layer (IGL) and malpositioning of the Purkinje cells that are normally found aligned beneath (Fig. 5A). The IGL contains the somata of the granule cells that have migrated inward from the external layer through the Purkinje cell layer (PCL) (9). The presence of the IGL in the mutant cerebellum indicated that failure of the Purkinje cells to form a monolayer did not affect the inward migration of the granule cells (Fig. 5A). Immunostaining of parasagittal sections of the cerebellum for calbindin, a well-characterized differentiation antigen expressed by Purkinje cells, confirmed that the PCL was highly disorganized in the mutant brain at P20 and demonstrated that ablation of MKK4 expression did not cause any dendritic arborization defect (Fig. 5A). In addition, we found that the size of the Purkinje cells was decreased by around 25% in the absence of MKK4.

To further characterize the defect in Purkinje cell positioning, sagittal sections of the cerebellum were immunostained for calbindin (red) and NeuN (green) to label Purkinje and granule cells, respectively, at various postnatal stages (Fig. 5B). In the control cerebellum, the thick sheet of Purkinje cells constituted at birth had dispersed by P10 into a monolayer that separated the molecular layer, a cell-poor lamina that contains the dendrites of the Purkinje cells and the parallel fiber of axons of the granule cells from the IGL (Fig. 5B). In contrast, Purkinje cells lacking MKK4 were unable to reorganize, with a significant number of them misplaced in the IGL by P6 (Fig. 5B). Consistent with the histological analysis of the brain (Fig. 5A), these data demonstrate that the malpositioning of the Purkinje cells did not prevent the inward migration of the granule cells.

Birth date analysis. We did not find any evidence that the loss of MKK4 caused increased apoptosis in the brain (data not shown). Thus, we explored the possibility that the misplacement of the Purkinje cells in the absence of MKK4 was correlated with birth date abnormalities. In mice, Purkinje cells are born in the ventricular zone of the cerebellar primordium between E11 and E13, at which time they exit the cell cycle to migrate toward the cerebellar plate. Therefore, timed pregnant females were injected with BrdU 11 and 13 days postcoitum. The offspring were sacrificed 7 days after birth. Nuclei of Purkinje cells that had incorporated the label while undergoing cell division at the time of injection were detected by BrdU

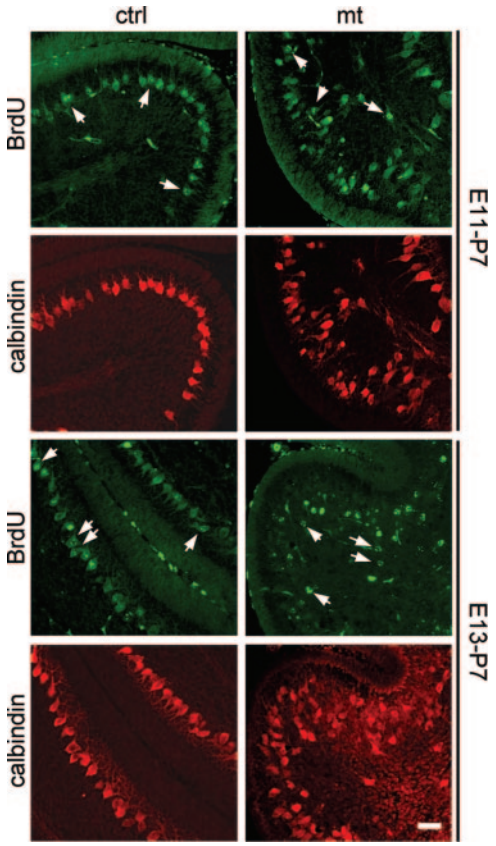

FIG. 6. Purkinje cell birth date analysis. Embryos were labeled with BrdU in utero at E11 and E13 and sacrificed at P7. Early-born (E11) and late-born (E13) Purkinje cells were detected by immunostaining them with a BrdU antibody. The arrows mark the BrdU-positive Purkinje cells. Scale bar, 50 μm.

immunoreactivity (Fig. 6). Both early-born (E11) and late-born (E13) Purkinje cells were found misplaced in the PCL, indicating that the malpositioning of the Purkinje cells was independent of their birth dates.

Although the gross anatomy of the mutant cortex showed no discernible anomaly at P20 (Fig. 4A), a similar analysis was performed in the cerebral cortex to test whether the absence of MKK4 affected radial migration, a process known to require JNK (22). Postmitotic neurons generated in the ventricular zone migrate radially toward the pial surface following the typical "inside-out" spatiotemporal sequence (37). Thus, early-born neurons reside deep in the cortex while those born late migrate past the existing layers of cells to form the upper layers. Embryos were labeled in utero with BrdU at the E14 or at E16 stage of gestation. Control experiments showed that the wild-type and mutant cells incorporated BrdU labeling to the same extent (see Fig. S1 in the supplemental material). As expected in the control mice, early-born neurons (E14) were found deep in the cortex (layers V and VI) (Fig. 7A and B), while late-born neurons (E16) were predominantly in the superficial cortex (layers I and II) (Fig. 7C and D). The kinetics of radial migration was notably different in the absence of MKK4. In the control mice, the majority of the early-born neurons (brightly labeled $BrdU^+$ cells) were positioned in the lower layers of the cortex at P1, while in the mutant mice, they were mostly in the upper layers (Fig. 7A, E14 to P1). This suggested a delay in the radial movement of late-born neurons (speckled $BrdU^+$ cells), as they showed an impediment to migration past the existing deep layers of the cortex. Consistent with this view, late-born mutant neurons (brightly labeled $BrdU^+$ cells) at P1 were still observed in the lower layers while most of them had already migrated to the upper layers in the control cortex (Fig. 7C, E16 to P1). Examination of the mutant cortex at P7 showed that the distributions of both early- and late-born neurons were comparable to those of controls (Fig. 7B, E14 to P7, and Fig. 7D, E16 to P7). Based on these data, we concluded that the absence of MKK4 transiently delayed the radial migration of late-born neurons without affecting the lamination of the cerebral cortex.

Loss of MKK4 does not affect radial glial-fiber formation. Migration of postmitotic neurons along radial glial fibers is the prevalent mode of neuronal movement in the developing mammalian brain (38). Immunohistochemical analysis of saggital sections of cortices confirmed that early on, the radial glial cells with elaborated long processes were immunopositive for nestin, a marker of undifferentiated neuroepithelial cells (Fig. 8). Parallel fibers that projected radially across the emerging cortex toward the meninges, where glial endfeet form, were detected in both the control and the mutant cerebra at embryonic and postnatal stages (Fig. 8A). Similarly, the loss of MKK4 did not prevent the establishment of the Bergmann glia fascicules, as detected by immunoreactivity against the nestin antibody at P1 and P3 (Fig. 8B). Collectively, these results indicated that the absence of MKK4 did not affect the integrity of the radial glial architecture to support neuronal migration. In addition, we found that the transmission of the Reelin signal, which is crucially important for instructing neurons to move along radial glial fibers (41), was unaffected by the deletion of the *mkk4* gene (see Fig. S2 in the supplemental material). Therefore, the migratory defect is most likely a cell-autonomous effect of the deletion of the *mkk4* gene in neurons.

Identification of target genes downstream of MKK4. To shed light on the molecular mechanism by which MKK4 affects neuronal migration and positioning, we performed microarray analysis using mRNAs isolated from control and mutant E14 embryonic forebrains. This analysis demonstrated that the loss of MKK4 significantly altered the expression of Rho-activated kinase (ROCK) and p21-activated kinase (PAK), which are both involved in the regulation of actin dynamics, such as stress fiber formation and focal adhesion turnover (1, 4). These changes were confirmed by real-time PCR experiments (Fig. 9A). The results showed a significant decrease in *ROCK1* (60%; $P < 0.001$) and *PAK2* (70%; $P < 0.001$), and to a lesser extent in *ROCK2* (35%; $P < 0.001$) and *PAK1* (20%; $P < 0.01$), transcripts in the mutant compared with the control forebrains. In contrast, MKK4 was not required ($P > 0.05$) for normal expression of LIM kinases 1 and 2, which stabilize filamentous actin downstream of ROCK and PAK (13, 31) (Fig. 9A). Similarly, expression of focal adhesion kinase, a nonreceptor cytoplasmic tyrosine kinase that modulates cell migration in response to adhesive interactions between the cell and the extracellular matrix, was unchanged in the absence of MKK4, demonstrating the selective effect of *mkk4* gene disruption on

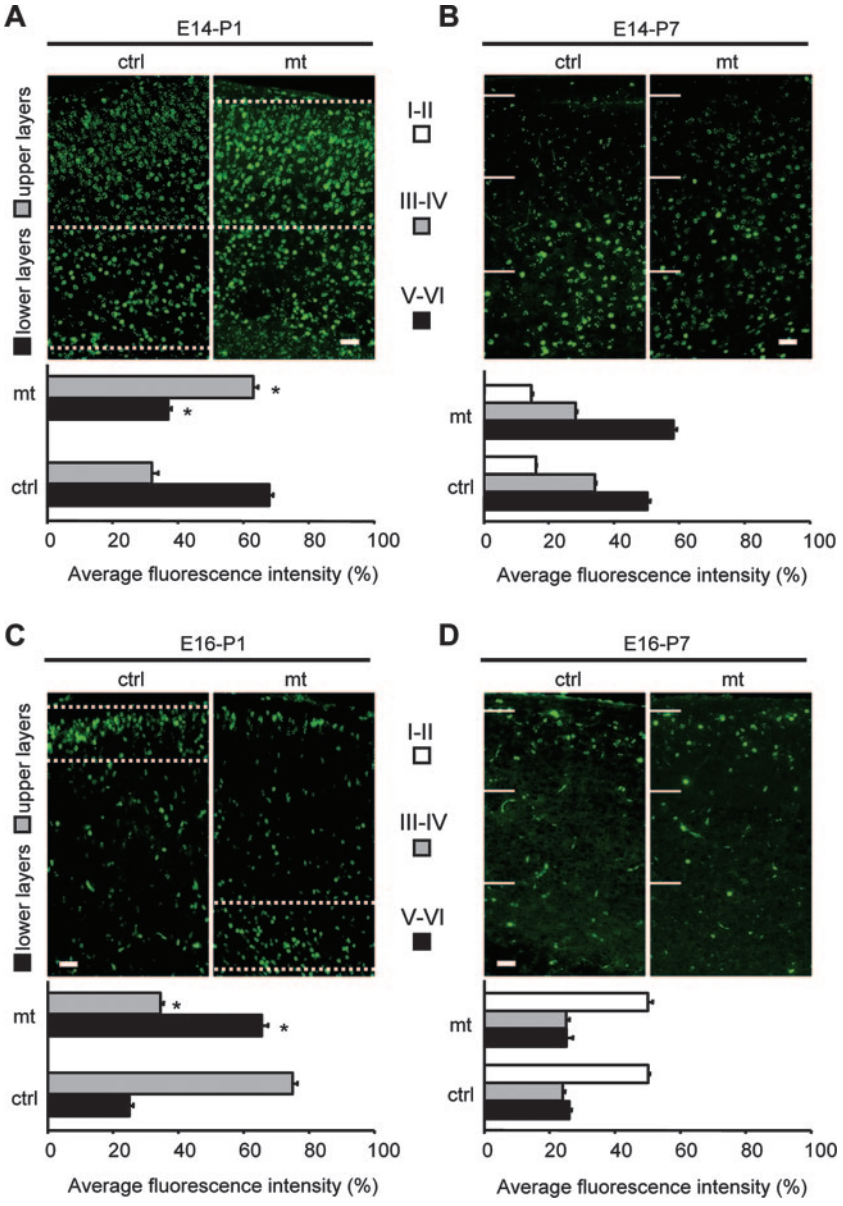

FIG. 7. Absence of MKK4 delays radial migration in the cerebral cortex. Pregnant mice were injected at 14 or 16 days postcoitum, and the distributions of early-born (E14) (A and B) and late-born (E16) (C and D) neurons in the cerebral cortices of the offspring at P1 (A and C) or P7 (B and D) were determined by immunostaining them with a BrdU antibody. BrdU immunoreactivity shows the progressive migration of the early-born neurons from the upper layers toward the deeper layers (V and VI) of the cortex. Conversely, the late-born neurons (E16) were predominantly found in the superficial cortex (layers I and II). Delayed radial migration in the absence of MKK4 was notable at P1, when most of the early-born neurons were in the upper layers while late-born neurons had not yet started their migration toward the deeper cortical layers. The extent of migration was estimated by measuring fluorescence intensities in distinct layers of the cerebral cortex. Intensities relative to the total fluorescence were calculated and plotted in graphs with standard errors ($n = 3$ animals). *, $P < 0.01$, indicating a significant difference in fluorescence intensity between control and mutant cortices. Scale bar, 50 μm.

gene expression (data not shown). Consistent with *mekk4* gene deletion (44), loss of MKK4 caused a relatively moderate but statistically significant ($P < 0.01$) increase in filamin A (FLN-A) expression (Fig. 9A). In addition, we found that the expression of kinesin 2 and β2 tubulin, two fundamental components of the intracellular transport of organelles (20), was greatly enhanced in the absence of MKK4 (Fig. 9A).

Phosphorylation of MAP1B and NF-H is impaired in the absence of MKK4. The microtubule-associated proteins MAP1B, MAP2, and double cortin (DCX) are essential for normal brain development (12, 17, 25, 33, 47, 48). Their ability to control microtubule dynamics is regulated upon phosphorylation by a number of protein kinases, including JNK (3, 8, 16, 22). We found no evidence that MKK4 was implicated in mediating DCX or MAP2 phosphorylation (see Fig. S3 in the supplemental material). In contrast, absence of MKK4 almost completely abolished the phosphorylation of MAP1B (Fig. 9B). This was demonstrated by immunoblot analysis using the

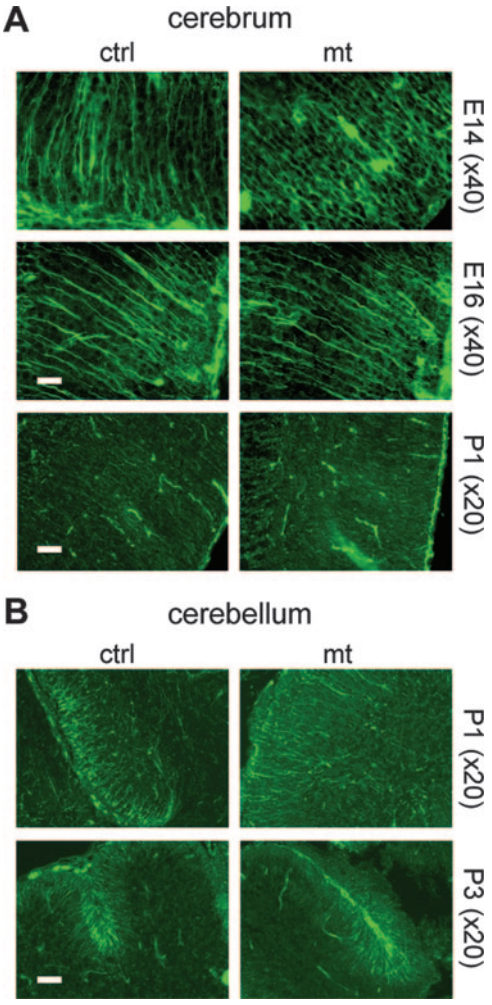

FIG. 8. The loss of MKK4 does not affect the architecture of the radial glial fibers. Sagittal sections of control (ctrl) and mutant (mt) cortices at various embryonic and postnatal stages were immunostained with antibodies to nestin to visualize radial glial fibers. The radial glia in the cerebra (A) and in the cerebella (B) of both genotypes formed a regular network with fibers extending through the cortical plate to the meningeal-cell layer. Scale bars: ×20, 50 μm; ×40, 25 μm.

SMI31 antibody, which detects the phosphorylated MAP1B isoform, which displays reduced microtubule-stabilizing activity, only in the control extracts. A pan-anti-MAP1B antibody (N19) revealed that the level of MAP1B expression was unaffected by the loss of MKK4 (Fig. 9B). We concluded that MKK4-mediated MAP1B phosphorylation was likely to be part of the mechanism by which MKK4 reduces microtubule stabilization to promote cell motility.

Similarly, SMI31 was unable to detect the phosphorylated form of NF-H in the mutant samples (Fig. 9B). This correlated with a strong immunoreactivity of the Purkinje cells and of neurons in layer V in the mutant cortices against SMI32, an antibody that specifically recognizes the nonphosphorylated epitope of NF-H (Fig. 9C). The defective phosphorylation of NF-H in brain extracts lacking MKK4 was further confirmed by the absence of an electrophoretic migratory shift of the protein analyzed by SDS-PAGE using a monoclonal antibody (N52) that detects both the hypo- and hyperphosphorylated forms of NF-H (Fig. 9B). Together, these results provide strong genetic evidence that MKK4 is required for mediating NF-H phosphorylation.

DISCUSSION

Overall, this study has increased our understanding of the physiological function of the JNK signaling pathway by allowing the functional effect of loss of JNK activation to be examined as opposed to loss of expression. The requirement for MKK4 to activate JNK in the nervous system can be explained by the distinct specificity of MKK4 and MKK7 for the Tyr and Thr residues within the T-X-Y motif of JNK (15, 28, 29). Consequently, both activators might be required to induce maximal activation of JNK. Alternatively, MKK4 may be the main JNK activator in the brain during development. Indeed, the overall level of expression of *mkk4* mRNA in the embryo is much higher than that of *mkk7*, which is found mainly in epithelial tissues (35, 54). Furthermore, we found that MKK7 expression is lower in embryonic than in postnatal stage. The analysis of the effect of the targeted deletion of the *mkk7* gene in the CNS will be essential to distinguish between these two possibilities and to clarify whether MKK4 and MKK7 have distinct functions in the brain during embryogenesis. In addition, we found that p38 MAPK activity was reduced in the absence of MKK4. This is consistent with the physiological role of MKK4 in mediating p38 MAPK activation in response to stress (5).

Impaired JNK activity caused by *mkk4* gene deletion was not correlated with the defect in neuronal apoptosis and exencephaly displayed by the *jnk1*$^{-/-}$ *jnk2*$^{-/-}$ mice (26, 43) or with the loss of telencephalic commissures, as observed in the brains of the *jnk1*$^{-/-}$ and *jip3*$^{-/-}$ mice (8, 24). Instead, the fibers forming the CC and the AC appeared swollen and defasciculated. A reduction in the thickness of the CC and AC was previously observed in the cerebra of embryos lacking the dual leucine zipper kinase (DLK), a member of the mixed-lineage kinases that function as a MEKK in the JNK signaling pathway (19). Furthermore, similar to the effect of *mkk4* gene disruption, the loss of DLK resulted in delayed neural-cell migration (19). However, in contrast to *jnk1* (3, 8) or *dlk* gene deletion (19), the disruption of the *mkk4* gene did not affect the phosphorylation of MAP2. We also found no difference in the phosphorylation of DCX in the brain in the embryonic or postnatal stage at three consensus sites for JNK (16, 19). Thus, although the regulation of MKK4 by DLK may constitute an important signaling pathway that contributes to the development of the telencephalon, it is possible that the loss of MKK4 and DLK selectively affects different JNK isoforms. Consequently, the remaining 20% of JNK activity in the MKK4 mutant brain may be sufficient for triggering the phosphorylation of a subset of JNK substrates displaying high affinity for JNK1.

The most striking phenotypic abnormality displayed by the brain-specific *mkk4*$^{-/-}$ mice was the inability of the Purkinje cells to organize in the typical linear position at the molecular layer-IGL boundary. Purkinje cells are the primary integrative neurons of the cerebellar cortex and provide its sole output (49). As a result, alteration in the PCL is often associated with

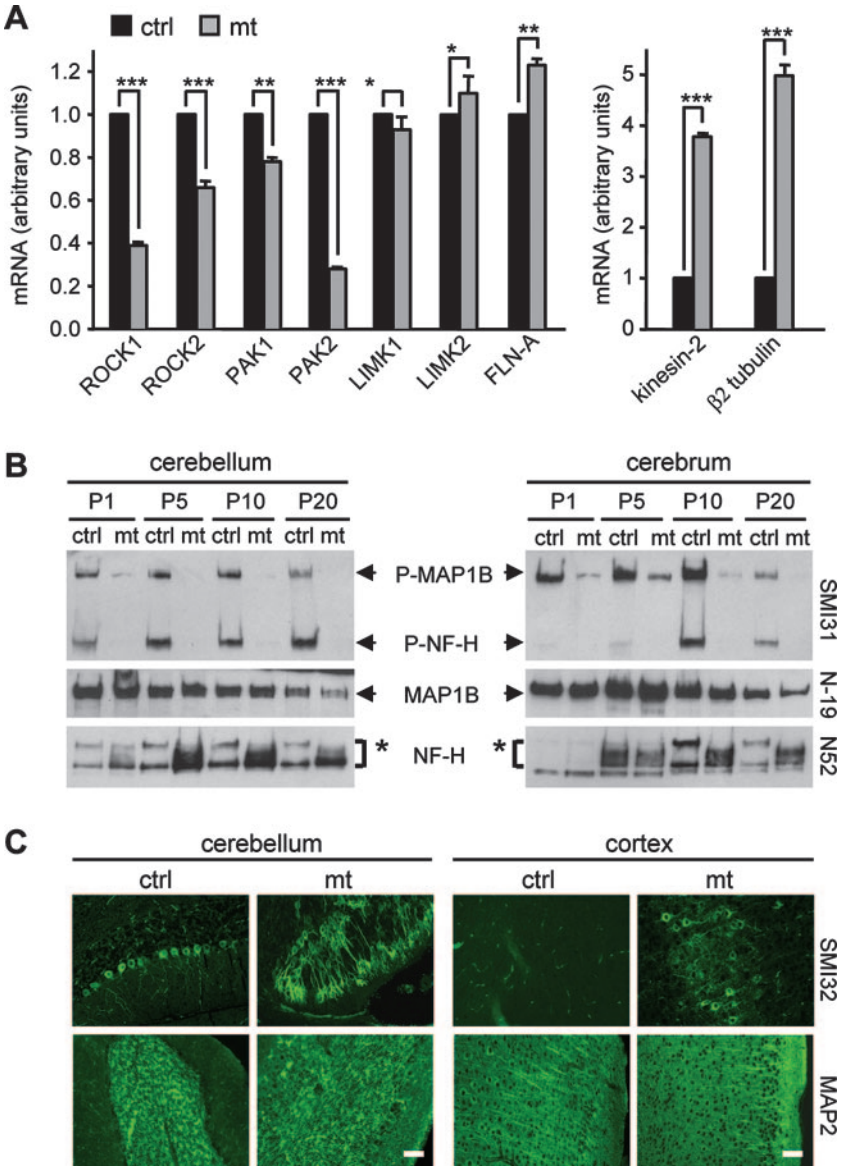

FIG. 9. Identification of downstream targets of MKK4. (A) Total RNAs were extracted from control (ctrl) and mutant (mt) E14 embryonic forebrains, and the amounts of various transcripts were measured by quantitative real-time PCR. The data are expressed relative (*n*-fold) to the mRNA extracted from the control brain and correspond to the means and standard errors of three independent experiments performed in triplicate. *P* values relative to the control sample are indicated by asterisks: ***, $P < 0.001$; **, $P < 0.01$; *, $P > 0.05$. (B) Phosphorylation of MAP1B and NF-H was examined by immunoblot analysis of brain extracts (20 μg) using antibodies against the phosphorylated forms of MAP1B and NF-H (SMI31). Absence of MKK4 was correlated with a specific defect in MAP1B and NF-H phosphorylation. Pan-antibodies to MAP1B (N19) and NF-H (N52) showed no significant difference in the expression levels of the proteins between the two genotypes. Note that the detection of phospho-NF-H (P-NF-H) by SMI31 in control extracts was correlated with the retarded mobility of the protein after SDS-PAGE. Similar results were obtained in two independent experiments. (C) Consistent with the defective phosphorylation of NF-H in the mutant extracts, cerebellar and cerebral cortices lacking MKK4 displayed strong immunoreactivity against SMI32, an antibody that specifically reacts with the nonphosphorylated form of NF-H. No difference was observed in the immunostaining of the control and mutant cortices with the anti-MAP2 antibody. Scale bar, 50 μm.

functional lesions of the cerebellum. Since the cerebellum acts as a coordination center using sensory inputs from the periphery to fine tune movement and balance (21), the defect in Purkinje cell positioning is likely to be the cause of the motor deficits displayed by the mutant animals. In addition to coordinating motion, MKK4 may also be involved in the higher cognitive functions of the cerebellum, such as motor learning (21). Overall, we conclude that the cerebellar defect associated with the loss of MKK4 is likely to be responsible for the early demise of the mutant mice.

To shed light on the biochemical mechanisms that account for the phenotypic abnormalities caused by MKK4 ablation, we searched for physiologically relevant substrates of JNK whose phosphorylation required MKK4. Consistent with the ability of MKK4 to activate JNK in both the cell body and processes of neurons (10), we found that the phosphorylation of both nu-

clear (c-Jun and ATF2) and cytosolic (MAP1B and NF-H) targets of JNK was impaired in the absence of MKK4. It is unlikely that the defect in c-Jun phosphorylation contributes to the abnormal phenotype of the MKK4 mutant mice because mutational removal of the JNK phosphorylation sites in c-Jun causes no obvious brain-developmental defect (2). In contrast, similar misplacement of Purkinje cells has been observed in the cerebella of *atf2*-, and *map1B*-deficient mice (17, 40). This suggests that MKK4-induced ATF2 and MAP1B phosphorylation by JNK may be critical for the organization of the PCL into a monolayer beneath the IGL.

The defective phosphorylation of MAP1B, together with abnormal gene regulation in the absence of MKK4, may also be responsible for delayed radial migration in the cerebral cortex. This is strongly supported by JNK-dependent phosphorylation of MAP1B, which leads to microtubule stabilization in migrating neurons (22), and by excess expression of FLN-A, which inhibits neuronal migration caused by *mekk4* gene deletion (44). The moderate increase in FLN-A expression in the absence of MKK4 is consistent with a delay rather than a block in cell motility. The down-regulation of ROCK and PAK in the mutant E14 embryonic forebrains may also contribute to the migration defect by affecting actin dynamics and subsequently the formation of stress fibers and focal adhesions (1, 4). In addition, reduced expression of ROCK may account in part for the effects of *mkk4* gene disruption on the development of the telencephalic commissures, since altered Rho signaling causes defects in the morphogenesis of commissural neurons (6, 7). Increased expression of kinesin-2 and β2 tubulin in the absence of MKK4 would be expected to affect the intracellular transport of organelles in axons and cellular morphology, which can also influence cell locomotion (20).

In contrast to MAP1B, very little is known about the functional effect of NF-H phosphorylation. NF-H is one of the five major types of intermediate filament proteins expressed in mature neurons (27). It is found heavily phosphorylated on its carboxy-terminal tail domain in axons. This was originally thought to be involved in determining axonal caliber (32). However, this suggestion was recently disputed by the phenotypic analysis of mice with targeted deletion of the C-terminal domain containing all of the phosphorylation sites (39). Alternatively, NF-H, together with MAP1B, may be required for the proper dendritic arborization of neurons, a process known to be controlled by JNK (3, 27, 42). This is consistent with the maximum phosphorylation of NF-H and MAP1B at a time (P10) when dendrites are actively formed in the cerebrum. An understanding of the implication of MKK4-dependent phosphorylation of NF-H and MAP1B in dendritic development may provide crucial information on how functional neural circuits in the brain are established. These results may also be relevant to increasing our knowledge of the role of JNK in neurodegenerative diseases associated with abnormal phosphorylation of NF-H, such as diabetic neuropathy (14).

ACKNOWLEDGMENTS

We are indebted to A. Nagy for kindly providing us with the R1 ES cells and to J. Ávila, O. Reiner, and R. Hawkes for their generosity in providing antibodies. We thank U. Müeller (Scripps Institute) for providing us with the nestin-Cre transgenic mice and A. Whitmarsh for critically reviewing the manuscript.

This work was supported by the BBSRC and a Lister Institute of Preventive Medicine Research Fellowship to C.T.

REFERENCES

1. **Amano, M., Y. Fukata, and K. Kaibuchi.** 2000. Regulation and functions of Rho-associated kinase. Exp. Cell. Res. **261:**44–51.
2. **Behrens, A., M. Sibilia, and E. F. Wagner.** 1999. Amino-terminal phosphorylation of c-Jun regulates stress-induced apoptosis and cellular proliferation. Nat. Genet. **21:**326–329.
3. **Björkblom, B., N. Östman, V. Hongisto, V. Komarovski, J.-J. Filén, T. A. Nyman, T. Kallunki, M. J. Courtney, and E. T. Coffey.** 2005. Constitutively active cytoplasmic c-Jun N-terminal kinase 1 is a dominant regulator of dendritic architecture: role of microtubule-associated protein 2 as an effector. J. Neurosci. **25:**6350–6361.
4. **Bokoch, G. M.** 2003. Biology of the p21-activated kinases. Annu. Rev. Biochem. **72:**743–781.
5. **Brancho, D., N. Tanaka, A. Jaeschke, J.-J. Ventura, N. Kelkar, Y. Tanaka, M. Kyuuma, T. Takeshita, R. A. Flavell, and R. J. Davis.** 2003. Mechanism of p38 MAP kinase activation in vivo. Genes Dev. **17:**1969–1978.
6. **Brouns, M. R., S. F. Matheson, K.-Q. Hu, I. Delalle, V. S. Caviness, Jr., J. Silver, R. T. Bronson, and J. Settleman.** 2000. The adhesion signaling molecule p190 RhoGAP is required for morphogenetic processes in neural development. Development **127:**4891–4903.
7. **Brouns, M. R., S. F. Matheson, and J. Settleman.** 2001. p190 RhoGAP is the principal Src substrate in brain and regulates axon outgrowth, guidance and fasciculation. Nat. Cell Biol. **3:**361–367.
8. **Chang, L., Y. Jones, M. H. Ellisman, L. S. B. Goldstein, and M. Karin.** 2003. JNK1 is required for maintenance of neuronal microtubules and controls phosphorylation of microtubule-associated proteins. Dev. Cell **4:**521–533.
9. **Chizhikov, V., and K. J. Millen.** 2003. Development and malformations of the cerebellum in mice. Mol. Genet. Metab. **80:**54–65.
10. **Coffey, E. T., V. Hongisto, M. Dickens, R. J. Davis, and M. J. Courtney.** 2000. Dual roles for c-Jun N-terminal kinase in developmental and stress responses in cerebellar granule neurons. J. Neurosci. **20:**7602–7613.
11. **Davis, R. J.** 2000. Signal transduction by the JNK group of MAP kinases. Cell **103:**239–252.
12. **Deuel, T. A. S., J. S. Liu, J. C. Corbo, S.-Y. Yoo, L. B. Rorke-Adams, and C. A. Walsh.** 2006. Genetic interactions between doublecortin and doublecortin-like kinase in neuronal migration and axon outgrowth. Neuron **49:**41–53.
13. **Edwards, D. C., L. C. Sanders, G. M. Bokoch, and G. N. Gill.** 1999. Activation of LIM-kinase by Pak1 couples Rac/Cdc42 GTPase signalling to actin cytoskeletal dynamics. Nat. Cell Biol. **1:**253–259.
14. **Fernyhough, P., A. Gallagher, S. A. Averill, J. V. Priestley, L. Hounsom, J. Patel, and D. R. Tomlinson.** 1999. Aberrant neurofilament phosphorylation in sensory neurons of rats with diabetic neuropathy. Diabetes **48:**881–889.
15. **Fleming, Y., C. G. Armstrong, N. Morrice, A. Paterson, M. Goedert, and P. Cohen.** 2000. Synergistic activation of stress-activated protein kinase 1/c-Jun N-terminal kinase (SAPK1/JNK) isoforms by mitogen-activated protein kinase kinase 4 (MKK4) and MKK7. Biochem. J. **352:**145–154.
16. **Gdalyahu, A., I. Ghosh, T. Levy, T. Sapir, S. Sapoznik, Y. Fishler, D. Azoulai, and O. Reiner.** 2004. DCX, a new mediator of the JNK pathway. EMBO J. **23:**823–832.
17. **González-Billault, C., J. A. Del Río, J. M. Ureña, E. M. Jiménez-Mateos, M. J. Barallobre, M. Pascual, L. Pujadas, S. Simó, A. La Torre, R. Gavin, F. Wandosell, E. Soriano, and J. Ávila.** 2005. A role of MAP1B in Reelin-dependent neuronal migration. Cereb. Cortex **15:**1134–1145.
18. **Graus-Porta, D., S. Blaess, M. Senften, A. Littlewood-Evans, C. Damsky, Z. Huang, P. Orban, R. Klein, J. C. Schittny, and U. Müller.** 2001. Beta1-class integrins regulate the development of laminae and folia in the cerebral and cerebellar cortex. Neuron **31:**367–379.
19. **Hirai, S., D. F. Cui, T. Miyata, M. Ogawa, H. Kiyonari, Y. Suda, S. Aizawa, Y. Banba, and S. Ohno.** 2006. The c-Jun N-terminal kinase activator dual leucine zipper kinase regulates axon growth and neuronal migration in the developing cerebral cortex. J. Neurosci. **26:**11992–12002.
20. **Hunter, A. W., and L. Wordeman.** 2000. How motor proteins influence microtubule polymerization dynamics. J. Cell Sci. **113:**4379–4389.
21. **Ito, M.** 1984. The cerebellum and neural control. Raven, New York, NY.
22. **Kawauchi, T., K. Chihama, Y. Nabeshima, and M. Hoshino.** 2003. The in vivo roles of STEF/Tiam1, Rac1 and JNK in cortical neuronal migration. EMBO J. **22:**4190–4201.
23. **Kayahara, M., X. Wang, and C. Tournier.** 2005. Selective regulation of c-*jun* gene expression by the mitogen-activated protein kinases via the TPA-responsive element and the myocyte enhancer factor 2 binding sites. Mol. Cell. Biol. **25:**3784–3792.
24. **Kelkar, N., M.-H. Delmotte, C. R. Weston, T. Barrett, B. J. Sheppard, R. A. Flavell, and R. J. Davis.** 2003. Morphogenesis of the telencephalic commissure requires scaffold protein JNK-interacting protein 3 (JIP3). Proc. Natl. Acad. Sci. USA **100:**9843–9848.
25. **Koizumi, H., T. Tanaka, and J. G. Gleeson.** 2006. Doublecortin-like kinase functions with doublecortin to mediate fiber tract decussation and neuronal migration. Neuron **49:**55–66.

26. **Kuan, C. Y., D. D. Yang, D. R. S. Roy, R. J. Davis, P. Rakic, and R. A. Flavell.** 1999. The Jnk1 and Jnk2 protein kinases are required for regional specific apoptosis during early brain development. Neuron **22:**667–676.
27. **Lariviere, R. C., and J.-P. Julien.** 2004. Functions of intermediate filaments in neuronal development and disease. J. Neurobiol. **58:**131–148.
28. **Lawler, S., Y. Fleming, M. Goedert, and P. Cohen.** 1998. Synergistic activation of SAPK1/JNK1 by two MAP kinase kinases in vitro. Curr. Biol. **8:**1387–1390.
29. **Lisnock, J.-M., P. Griffin, J. Calaycay, B. Frantz, J. Parsons, S. J. O'Keefe, and P. LoGrasso.** 2000. Activation of JNK3α1 requires both MKK4 and MKK7: kinetic characterization of in vitro phosphorylation JNK3α1. Biochemistry **39:**3141–3148.
30. **Livak, K. L., and T. D. Schmittgen.** 2001. Analysis of relative gene expression data using real-time quantitative PCR and the 2(-delta delta C(T)). Methods **25:**402–408.
31. **Maekawa, M., T. Ishizaki, S. Boku, N. Watanabe, A. Fujita, A. Iwamatsu, T. Obinata, K. Ohashi, K. Mizuno, and S. Narumiya.** 1999. Signaling from Rho to the actin cytoskeleton through protein kinases ROCK and LIM-kinase. Science **285:**895–898.
32. **Marszalek, J. R., T. L. Williamson, M. K. Lee, Z. S. Xu, P. N. Hoffman, M. W. Becher, T. O. Crawford, and D. W. Cleveland.** 1996. Neurofilament subunit NF-H modulates axonal diameter by selectively slowing neurofilament transport. J. Cell Biol. **135:**711–724.
33. **Meixner, A., S. Haverkamp, H. Wässle, S. Führer, J. Thalhammer, N. Kropf, R. E. Bittner, H. Lassmann, G. Wiche, and F. Propst.** 2000. MAP1B is required for axon guidance and is involved in the development of the central and peripheral nervous system. J. Cell Biol. **151:**1169–1178.
34. **Müller, U., D. Wang, S. Denda, J. J. Meneses, R. A. Pedersen, and L. F. Reichardt.** 1997. Integrin α8β1 is critically important for epithelial-mesenchymal interactions during kidney morphogenesis. Cell **88:**603–613.
35. **Nishina, H., C. Vaz, P. Billia, M. Nghiem, T. Sasaki, J. L. De la Pompa, K. Furlonger, C. Paige, C.-C. Hui, K.-D. Fischer, H. Kishimoto, T. Iwatsubo, T. Katada, J. R. Woodgett, and J. M. Penninger.** 1999. Defective liver formation and liver cell apoptosis in mice lacking the stress signaling kinase SEK1/MKK4. Development **126:**505–516.
36. **Raingeaud, J., A. J. Whitmarsh, B. Barrett, B. Derijard, and R. J. Davis.** 1996. MKK3- and MKK6-regulated gene expression is mediated by the p38 mitogen-activated protein kinase signal transduction pathway. Mol. Cell. Biol. **16:**1247–1255.
37. **Rakic, P.** 1972. Mode of cell migration to the superficial layers of fetal monkey neocortex. J. Comp. Neurol. **145:**61–83.
38. **Rakic, P.** 1990. Principles of neural cell migration. Experientia **46:**882–891.
39. **Rao, M. V., M. L. Garcia, Y. Miyazaki, T. Gotow, A. Yuan, S. Mattina, C. M. Ward, N. A. Calcutt, Y. Uchiyama, R. A. Nixon, and D. W. Cleveland.** 2002. Gene replacement in mice reveals that the heavily phosphorylated tail of neurofilament heavy subunit does not affect axonal caliber or the transit of cargoes in slow axonal transport. J. Cell Biol. **158:**681–693.
40. **Reimold, A. M., M. J. Grusby, B. Kosaras, J. W. U. Fries, R. Mori, S. Maniwa, I. M. Clauss, T. Collins, R. L. Sidman, M. J. Glimcher, and L. H. Glimcher.** 1996. Chondrodysplasia and neurological abnormalities in ATF-2-deficient mice. Nature **379:**262–265.
41. **Rice, D. S., and T. Curran.** 2001. Role of the Reelin signaling pathway in central nervous system development. Annu. Rev. Neurosci. **24:**1005–1039.
42. **Rosso, S. B., D. Sussman, A. Wynshaw-Boris, and P. C. Salinas.** 2005. Wnt signaling through Dishevelled, Rac and JNK regulates dendritic development. Nat. Neurosci. **8:**34–42.
43. **Sabapathy, K., W. Jochum, K. Hochedlinger, L. Chang, M. Karin, and E. F. Wagner.** 1999. Defective neural tube morphogenesis and altered apoptosis in the absence of both JNK1 and JNK2. Mech. Dev. **89:**115–124.
44. **Sarkisian, M. R., C. M. Bartley, H. Chi, F. Nakamura, K. Hashimoto-Torii, M. Torii, R. A. Flavell, and P. Rakic.** 2006. MEKK4 signaling regulates filamin expression and neuronal migration. Neuron **52:**789–801.
45. **Sauer, B.** 1998. Inducible gene targeting in mice using the Cre/Lox system. Methods **14:**381–392.
46. **Schwander, M., M. Leu, M. Stumm, O. M. Dorchies, U. T. Ruegg, J. Schittny, and U. Müller.** 2003. Beta1 integrins regulate myoblast fusion and sarcomere assembly. Dev. Cell **4:**673–685.
47. **Takei, Y., S. Kondo, A. Harada, S. Inomata, T. Noda, and N. Hirokawa.** 1997. Delayed development of nervous system in mice homozygous for disrupted microtubule-associated protein 1B (MAP1B) gene. J. Cell Biol. **137:**1615–1626.
48. **Teng, J., Y. Takei, A. Harada, T. Nakata, J. Chen, and N. Hirokawa.** 2001. Synergistic effects of MAP2 and MAP1B knockout in neuronal migration, dendritic outgrowth, and microtubule organization. J. Cell Biol. **155:**65–76.
49. **Voogd, J., J. Pardoe, T. H. Ruigrok, and R. Apps.** 2003. The distribution of climbing and mossy fiber collateral branches from the copula pyramidis and the paramedian lobule: congruence of climbing fiber cortical zones and the pattern of zebrin banding within the rat cerebellum. J. Neurosci. **23:**4645–4656.
50. **Wang, X., A. Destrument, and C. Tournier.** 2007. Physiological roles of MKK4 and MKK7: insights from animal models. Biochim. Biophys. Acta **1773:**1349–1357.
51. **Widmann, C., S. Gibson, M. B. Jarpe, and G. L. Johnson.** 1999. Mitogen-activated protein kinase: conservation of a three-kinase module from yeast to human. Physiol. Rev. **79:**143–180.
52. **Yang, D. D., C. Y. Kuan, A. J. Whitmarsh, M. Rincon, T. S. Zheng, R. J. Davis, P. Rakic, and R. A. Flavell.** 1997. Absence of excitotoxicity-induced apoptosis in the hippocampus of mice lacking the Jnk3 gene. Nature **389:**865–870.
53. **Yang, S., A. D. Sharrocks, and A. J. Whitmarsh.** 2003. Transcriptional regulation by the MAP kinase signaling cascades. Gene **320:**3–21.
54. **Yao, Z., K. Diener, X. S. Wang, M. Zukowski, G. Matsumoto, G. Zhou, R. Mo, T. Sasaki, H. Nishina, C. C. Hui, T. H. Tan, J. P. Woodgett, and J. M. Penninger.** 1997. Activation of stress-activated protein kinases/c-Jun N-terminal protein kinases (SAPKs/JNKs) by a novel mitogen-activated protein kinase kinase (MKK7). J. Biol. Chem. **272:**32378–32383.
55. **Zarubin, T., and J. Han.** 2005. Activation and signaling of the p38 MAP kinase pathway. Cell Res. **15:**11–18.